Materials Chemistry and Physics 163 (2015) 416–420

Contents lists available at ScienceDirect

Materials Chemistry and Physics

journal homepage: www.elsevier.com/locate/matchemphys

Growth, structural and magnetic characterization of Zn-substituted barium hexaferrite single crystals

D.A. Vinnik [a, *], A.S. Semisalova [b], L.S. Mashkovtseva [a], A.K. Yakushechkina [b], S. Nemrava [c], S.A. Gudkova [a, g], D.A. Zherebtsov [a], N.S. Perov [b, e], L.I. Isaenko [d, f], R. Niewa [c]

[a] South Ural State University, 454080, Lenin's Prospect 76, Chelyabinsk, Russia
[b] Lomonosov Moscow State University, Faculty of Physics, 119991, Leninskie Gory 1-2, Moscow, Russia
[c] University of Stuttgart, 70569, Pfaffenwaldring 55, Stuttgart, Germany
[d] Institute of Geology and Mineralogy Siberian Branch Russian Academy of Sciences, 630090, Ac. Koptyuga ave., Novosibirsk, Russia
[e] Baltic Federal University, 236041, Nevskogo Street 14 A, Kaliningrad, Russia
[f] Novosibirsk State University, Pirogova Street 2, 630090 Novosibirsk, Russia
[g] Moscow Institute of Physics and Technology (State University), 141700, Institutskiy per. 9, Dolgoprudny, Moscow Region, Russia

HIGHLIGHTS

- Growth of large Zn-substituted crystals $BaFe_{12-x}Zn_xO_{19}$.
- Zn-content controllable by flux composition.
- Zn substitution influence on the unit cell parameters.
- Decrease of coercivity, magnetization and Curie temperature upon Zn-substitution.

ARTICLE INFO

Article history:
Received 19 February 2015
Received in revised form
24 June 2015
Accepted 26 July 2015
Available online 4 August 2015

Keywords:
Crystal growth
Magnetic materials
Crystal structure
Magnetic properties

ABSTRACT

Zn-doped barium hexaferrite $BaFe_{12-x}Zn_xO_{19}$ ($0 \le x \le 0.065$) single crystals were grown from carbonate flux at temperatures below 1260 °C in order to study the effect of Zn-substitution on the structural and magnetic properties. Upon increasing Zn-content the lattice parameters increase to a small degree, due to a larger ionic size of Zn^{2+} as compared to Fe^{3+}. The saturation magnetization and coercivity of the studied crystals turns out to depend very sensitive on the level of Zn-substitution. A considerable coercivity decrease up to 30% was observed for samples with $x = 0.065$, while the Curie temperature was found to be comparably little influenced, dropping from 455 °C for the undoped compound to 445 °C for the maximum x obtained. We demonstrate the possibility to use the carbonate flux growth method for producing hexaferrite crystals and tune their functional properties via doping with zinc.

1. Introduction

The interest in magnetic materials has historically been driven by use to create permanent magnets and high density magnetic recording storage devices. In the last decade, it has undergone significant changes due to the new opportunities for application of the unique properties of magnetic materials.

An example of such material is barium hexaferrite (M-type barium ferrite). The possibility to use hexaferrites in new applications explains the exponentially increasing degree of interest in these materials, which is ongoing today [1]. The structural and magnetic properties of barium hexaferrites were found to be strongly dependent on the fabrication method as well as on the substitution of Fe with ions of different nature and concentration (doping). In literature, results of comprehensive studies on modifying the properties by substitution of iron atoms in the magnetoplumbite-type $BaFe_{12}O_{19}$ are available [2–28]. Such functional magnetic characteristics as coercivity and Curie temperature

* Corresponding author.
E-mail addresses: denisvinnik@gmail.com (D.A. Vinnik), semisalova@magn.ru (A.S. Semisalova), l2787@yandex.ru (L.S. Mashkovtseva), yako.msu@yandex.ru (A.K. Yakushechkina), nemrava@iac.uni-stuttgart.de (S. Nemrava), svetlanagudkova@yandex.ru (S.A. Gudkova), zherebtsov_da@yahoo.com (D.A. Zherebtsov), perov@magn.ru (N.S. Perov), lisa@igm.nsc.ru (L.I. Isaenko), iacniewa@iac.uni-stuttgart.de (R. Niewa).

http://dx.doi.org/10.1016/j.matchemphys.2015.07.059
0254-0584/

can be significantly changed by doping with magnetic and non-magnetic metals [29–31]. The modification of $BaFe_{12}O_{19}$ by doping makes it possible to obtain unique and previously unknown properties of this material, which leads to the development of new applications. One example of such newly arising applications may be the use of barium hexaferrite as microwave absorbing material [32].

Currently, most commonly used materials for microwave absorbers are ferrite spinels with cubic crystal structure. However, the use of those spinels at frequencies of about 2 GHz is limited due to Snoek's limit [33–35]. Hexagonal ferrites with magnetoplumbite structure exhibit higher resonance frequency and higher microwave permeability and are thus expected to be more effective in the higher frequency range [36].

So far, the effect of Zn substitution on the properties of barium hexaferrite is poorly studied, although several reports can be found in literature [4,18–20,37–41]. Different cations or combinations of cations have been used to substitute the Fe^{3+} ions to reduce the grain size and high magnetic uniaxial anisotropy field of $BaFe_{12}O_{19}$ without affecting the saturation magnetization M_s for applications in high-density magnetic recording and microwave absorption devices [36]. For example, samples $BaFe_{12-2x}Zn_xTi_xO_{19}$ ($0 \le x \le 0.6$) were produced by mechanical milling. Upon increasing substitution of Fe a reduction can be observed in both the intrinsic coercivity, H_{ci}, and the remanent magnetization, M_r, whereas the saturation magnetization, M_s, diminishes gradually, having a maximum at $x = 0.3$. The Curie temperature was also found to be decreasing with x. The average temperature coefficient of H_c for samples $BaFe_{12-2x}Co_{x/2}Zn_{x/2}Sn_xO_{19}$ ($x = 0.0–0.6$) grown by co-precipitation/molten salt method decreases with x [21].

Since the information about the influence of solely Zn doping on the structure and functional properties of barium hexaferrites is sparse in literature, especially for case of flux grown crystals, this cation was chosen as an object for a detailed study of the substitution effect on the properties.

2. Experimental part

Crystals of Zn-substituted barium hexaferrites were grown from flux [42] composed of iron oxide (γ-Fe_2O_3), zinc oxide (ZnO), barium carbonate ($BaCO_3$) and sodium carbonate (Na_2CO_3) of 99.5% purity. Compositions of the batches are listed in Table 1.

The initial mixture was ground in an agate mortar, filled into a 30 mL platinum crucible and placed in a resistive furnace. The details can be found elsewhere [43,44]. Heating was controlled by a type B thermocouple and a precision thermocontroller RIF-101. The furnace was maintained at 1260 °C for 4 h followed by cooling to 900 °C with a rate of 4.5 K/h. The solidified material after cooling to room temperature was leached in hot nitric acid to separate the crystals.

The samples composition was determined using transmission electron microscope JEOL JSM7001F with energy-dispersive spectrometer Oxford INCA X-max 80 for elemental analysis. Powder X-ray diffraction analyses of powdered crystals was performed on a Rigaku Ultima IV diffractometer in the angular range from 10° to 80° with the speed of 0.5°/min using CuK_α radiation.

Single crystal X-ray diffraction was carried out using a four-circle diffractometer NONIUS κ-CCD, Bruker AXS at ambient temperature with monochromatic MoK_α radiation. Structural refinements were performed with isotropic displacement factors for the oxygen atoms to reduce the number of variables.

The Curie temperature was determined using differential scanning calorimetry on a Netzsch 449C Jupiter thermal analyzer. The samples were placed into a crucible and heated in air at a rate of 2 K/min up to 800 °C. The phase transition temperature was determined using the peak positions in heating and cooling cycles.

For further investigations, ground powders were sealed in plastic capsules with a maximum total weight of 9 mg. Magnetic properties were studied using vibrating sample magnetometer LakeShore 7407 in magnetic field up to 1.6 T at room temperature.

3. Results and discussion

High quality single crystals of $BaFe_{12-x}Zn_xO_{19}$ with Zn contents varying in the range $0 \le x \le 0.065$ were successfully grown from flux (see Table 1). We were able to perform the fabrication of samples at a temperature of 1260 °C, which is significantly lower than in the case of other crystal growth methods [45]. Similar to other transition metal substitutions like Ti, Co, Ni, Cu, or W, the doping level of Zn in barium hexaferrite crystals can be varied using different initial concentrations of the dopant in the batch [13,26,29,31,42]. The correlation of Zn concentration in the melt and in the crystals is shown in Fig. 1. Several selected hexagonal shaped crystals with size up to 7 mm are shown in Fig. 2.

The unit cell parameters of Zn-substituted barium hexaferrite crystals are summarized in Table 2 and compared with published

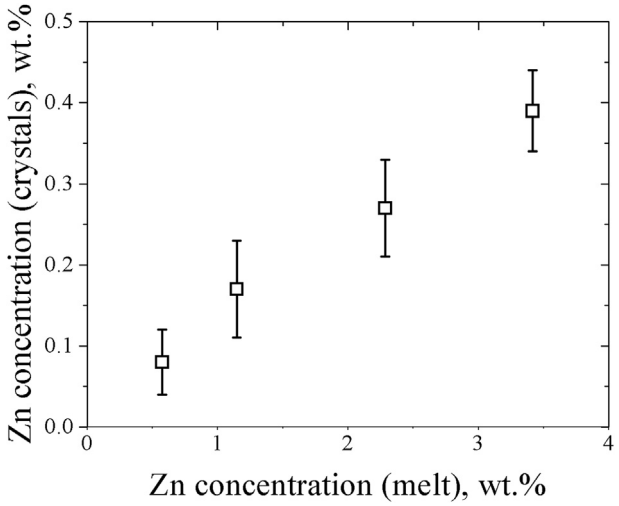

Fig. 1. Correlation of Zn-concentration in the melt and in the hexaferrite crystals.

Table 1
Composition of batches for ferrite crystal growth.

#	Target composition	Components concentration [wt.%]				Crystal composition
		ZnO	Fe_2O_3	$BaCO_3$	Na_2CO_3	
1	$BaFe_{12}O_{19}$	–	0.67465	0.13895	0.18640	$BaFe_{12}O_{19}$
2	$BaFe_{11.875}Zn_{0.125}O_{19}$	0.00715	0.66642	0.13870	0.18773	$BaFe_{11.985}Zn_{0.015}O_{19}$
3	$BaFe_{11.75}Zn_{0.25}O_{19}$	0.01427	0.65823	0.13845	0.18905	$BaFe_{11.975}Zn_{0.025}O_{19}$
4	$BaFe_{11.5}Zn_{0.5}O_{19}$	0.02844	0.64192	0.13796	0.19168	$BaFe_{11.955}Zn_{0.045}O_{19}$
5	$BaFe_{11.25}Zn_{0.75}O_{19}$	0.04251	0.62573	0.13747	0.19429	$BaFe_{11.935}Zn_{0.065}O_{19}$

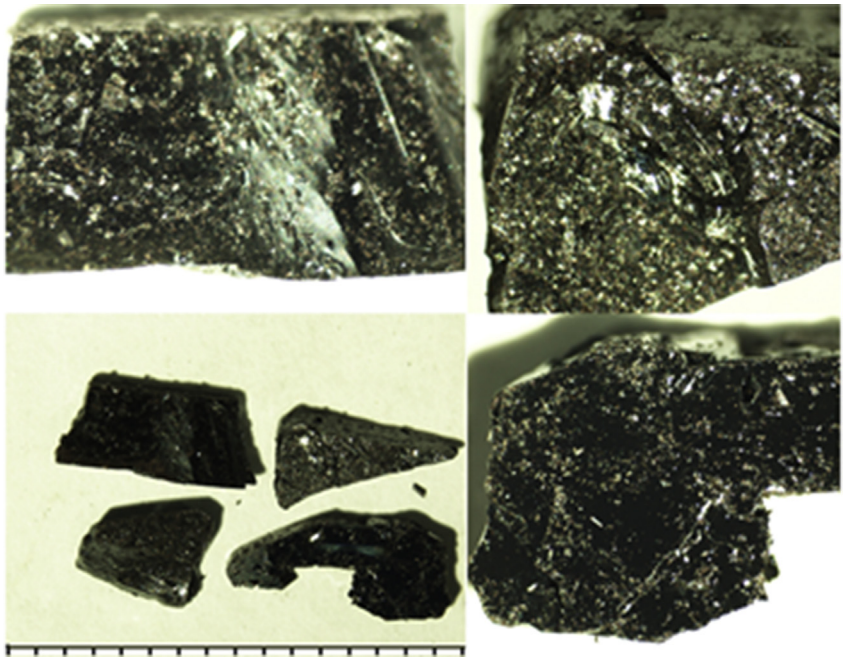

Fig. 2. $BaFe_{12-x}Zn_xO_{19}$ crystals obtained from flux composed of iron oxide (γ-Fe_2O_3), zinc oxide (ZnO), barium carbonate ($BaCO_3$) and sodium carbonate (Na_2CO_3) (left bottom scale is in mm).

Table 2
Unit cell parameters, Curie temperature and saturation magnetization values of Zn-doped hexaferrites in comparison with literature data for pure $BaFe_{12}O_{19}$ [31,46,48–50].

No.	Composition	a [Å]	c [Å]	V [Å^3]	T_C [°C]	M_s [emu/g]	H_c [Oe]
[46]	$BaFe_{12}O_{19}$	5.893	23.194	697.5	–	–	–
[48]	$BaFe_{12}O_{19}$	–	–	–	457	–	–
[49]	$BaFe_{12}O_{19}$	–	–	–	–	72	6700
[50]	$BaFe_{12}O_{19}$	–	–	–	–	59	360
1 [31]	$BaFe_{12}O_{19}$	5.8929(4)	23.194(2)	697.54(6)	455	71	363
2	$BaFe_{11.985}Zn_{0.015}O_{19}$	5.8930(4)	23.1937(15)	697.54(6)	452	64.83	325
3	$BaFe_{11.975}Zn_{0.025}O_{19}$	5.8939(6)	23.1972(22)	697.87(10)	450	62.89	303
4	$BaFe_{11.955}Zn_{0.045}O_{19}$	5.8941(5)	23.1992(18)	697.98(8)	448	61.87	262
5	$BaFe_{11.935}Zn_{0.065}O_{19}$	5.8949(4)	23.2031(15)	698.27(6)	445	54.4	259

data for pure $BaFe_{12}O_{19}$, including one pure sample obtained from the same carbonate flux technique as applied for growth of the Zn containing crystals [31,46]. There is a very small increase of both hexagonal lattice parameters a and c, and consequently V when x increases (Fig. 3). The tiny changes in the unit cell parameters are

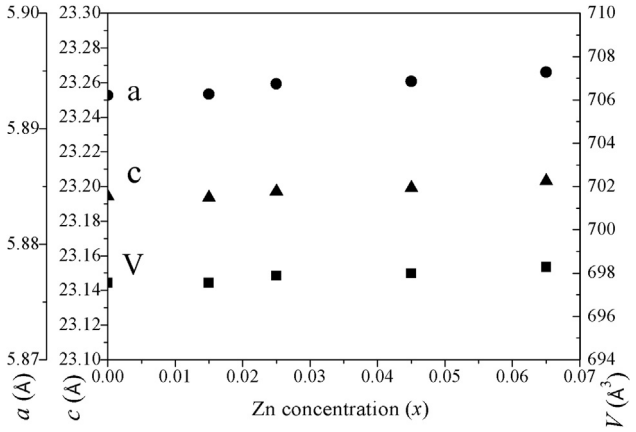

Fig. 3. Dependence of unit cell parameters a (Å), c (Å) and V (Å^3) of $BaFe_{12-x}Zn_xO_{19}$ on the Zn-content x.

well explained by the minute maximum doping level with Zn in the samples. Due to the larger size of Zn^{2+} ions compared to Fe^{3+} ions (e.g., $r(Fe^{3+})$ = 0.63 Å; $r(Zn^{2+})$ = 0.74 Å for CN = 4 and $r(Fe^{3+})$ = 0.785 Å (high-spin); $r(Zn^{2+})$ = 0.88 Å with CN = 6 [47]) an increasing unit cell is readily understood. For substitution with similarly larger Ni^{2+} and Co^{2+} ions we have recently observed analogously increasing unit cell parameters, however, followed by a decreasing unit cell volume with $x > 0.09$, probably related to the necessity of formation of oxygen vacancies for charge balance [26]. In case of substitution with higher-charged, but smaller Ti^{4+} ions, for comparison, an initial increase in unit cell parameters is related to reduction of Fe^{3+} to larger size Fe^{2+} ions, which only starts to be compensated above a degree of substitution of $x > 0.75$ due to formation of vacancies in the metal substructure [13].

Magnetic hysteresis loops measured at room temperature are presented in Fig. 4. The functional magnetic parameters such as Curie temperature, saturation magnetization and coercivity are also summarized in Table 2. Literature data of pure $BaFe_{12}O_{19}$ concern a wide variety of different synthesis techniques of studied samples, thus some properties cover large ranges [31,48–50]. For the crystals presented here, all three characteristics decrease with increasing Zn content. The largest change is observed for magnetization and coercivity values with almost 30% decrease, while the Curie temperature is found to change only by up to about 3% (Fig. 5).

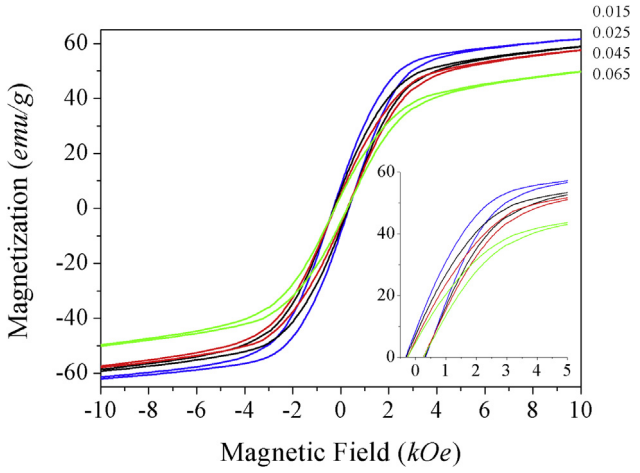

Fig. 4. Hysteresis loops of substituted barium hexaferrite samples with different Zn concentrations measured at room temperature.

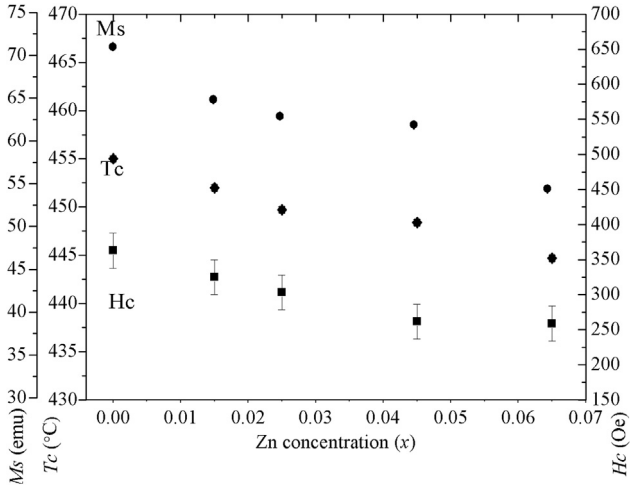

Fig. 5. Dependence of saturation magnetization, Curie temperature and coercive field of $BaFe_{12-x}Zn_xO_{19}$ on the Zn-content x.

Pure barium hexaferrite $BaFe_{12}O_{19}$ is an antiferromagnet with two sublattices of Fe ions: The spins at Fe located at the crystallographic sites $4f_1$ (Fe(3)) and $4f_2$ (Fe(4)) arrange antiparallel to those at $2a$ (Fe(1)), $2b$ (respectively $4e$, Fe(2)) and $12k$ (Fe(5)). According to earlier studies Zn ions occupy exclusively one crystallographic site ($4f_1$), which is located in tetrahedral coordination of oxide ions [20,41,51,52]. The exclusive occupation of Zn at a tetrahedrally coordinated site rather than those in octahedral environments in ferrites was earlier described [53,54]. Accordingly, for the magnetoplumbite structure, in addition to $4f_1$ only the $2b$ site might be considered for additional occupation with Zn^{2+}. Even a minute substitution with Zn^{2+} carrying no local magnetic moment leads to disturbance of the magnetic arrangement in its vicinity and a misbalance of Fe^{2+} and Fe^{3+} ions, which causes the magnetic properties change. The decrease of the coercivity with increasing Zn concentration can be explained as the result of decreasing magnetocrystalline anisotropy of the samples. The saturation magnetization depends on the superexchange interaction, which is sensitive to the interatomic distances and angles in the oxoferrate substructure. Substitution of Fe^{3+} by the larger Zn^{2+} leads to a decreasing exchange interaction and thus to a decreasing M_s. Above a Zn concentration of $x = 0.04$ the saturation magnetization decrease becomes more appreciable (Fig. 5). In the current investigation it was detected that a higher influence on the properties appears for concentration exceeding $x = 0.04$.

4. Conclusions

Zn-substituted barium ferrite single crystals $BaFe_{12-x}Zn_xO_{19}$ (x up to 0.065) with size up to 7 mm were grown from flux composed of iron oxide, zinc oxide and barium and sodium carbonates. This method can be used at temperatures significantly lower than for other fabrication techniques. The influence of Zn concentration on the structural and magnetic properties was studied. The lattice parameters were found to be slightly increasing with concentration of the dopant. Zn substitution significantly effects the coercivity and magnetization of barium hexaferrite, while the Curie temperature was shown to be nearly constant over the whole range of doping. The study shows the possibility to tune the magnetic properties including the magnetocrystalline anisotropy of $BaFe_{12}O_{19}$ in wide range via doping with zinc.

Acknowledgments

The work at SUrSU was supported by the National Research University program. Additionally the work was partially performed using equipment of MIPT Centers of Collective Usage and with financial support from the Ministry of Education and Science of the Russian Federation (Grant No. RFMEFI59414X0009). Financial support of RFBR (No. 13-02-12443) is acknowledged.

Appendix A. Supplementary data

Supplementary data related to this article can be found at http://dx.doi.org/10.1016/j.matchemphys.2015.07.059.

References

[1] R.C. Pullar, Hexagonal ferrites: a review of the synthesis, properties and applications of hexaferrite ceramics, Prog. Mater. Sci. 57 (2012) 1191–1334.
[2] X.B. Gelabert, M.G. del Muro, J. Tejada, H. Pfeiffer, P. Görnert, E. Sinn, Static magnetic properties of nanocrystalline Co–Ti doped barium ferrite $BaFe_{12-2x}Co_xTi_xO_{19}$ (x = 0.8), IEEE Trans. Magn. 30 (1994) 708–710.
[3] F.L. Wei, H.V. Fang, C.K. Ong, C.S. Wang, Z. Yang, Magnetic properties of $BaFe_{12-2x}Zn_xZr_xO_{19}$ particles, J. Appl. Phys. 87 (2000) 8636–8639.
[4] J. Sláma, A. Grusková, M. Papánová, D. Kevická, V. Jančárik, R. Dosoudil, G. Mendoza-Suárez, A. González-Angeles, Properties of M-type barium ferrite doped by selected ions, J. Electr. Eng. 56 (2005) 21–25.
[5] Z. Haijun, L. Zhichao, M. Chenliang, Y. Xi, Z. Liangying, W. Mingzhong, Preparation and microwave properties of Co- and Ti-doped barium ferrite by citrate sol-gel process, Mater. Chem. Phys. 80 (2003) 129–134.
[6] P.A. Mariño-Castellanos, A.C. Moreno-Borges, G. Orozco-Melgar, J.A. García, E. Govea-Alcaide, Structural and magnetic study of the Ti^{4+}-doped barium hexaferrite ceramic samples: theoretical and experimental results, Phys. B 406 (2011) 3130–3136.
[7] P. Quiroz, B. Halbedel, Synthesis and characterization of Ti-doped barium hexaferrite powders by glass crystallization technique, in: 54th International Scientific Colloquium, Ilmenau University of Technology, 2009.
[8] D. Chen, Y. Liu, Y. Li, K. Yang, H. Zhang, Microstructure and magnetic properties of Al-doped barium ferrite with sodium citrate as chelate ligand, JMMM 337–338 (2013) 65–69.
[9] V.N. Dhage, M.L. Mane, A.P. Keche, C.T. Birajdar, K.M. Jadhav, Structural and magnetic behaviour of aluminium doped barium hexaferrite nanoparticles synthesized by solution combustion technique, Phys. B 406 (2011) 789–793.
[10] V.I. Kostenko, T.G. Chamor, L.V. Chevnyuk, Ferromagnetic resonance in epitaxial films of Al-substituted barium hexaferrite, Ukr. J. Phys. 50 (2005) 265–267.
[11] I. Harward, Y. Nie, D. Chen, J. Baptist, M.J. Shaw, E.J. Liskova, S. Visnovsky, P. Siroky, M. Lesnak, J. Pistora, Z. Celinski, Physical properties of Al doped Ba hexagonal ferrite thin films, J. Appl. Phys. 113 (2013) 043903.
[12] Y. Li, R. Liu, Z. Zhang, C. Xiong, Synthesis and characterization of nanocrystalline $BaFe_{9.6}Co_{0.8}Ti_{0.8}M_{0.8}O_{19}$ particles, Mater. Chem. Phys. 64 (2000) 256–259.
[13] D.A. Vinnik, D.A. Zherebtsov, L.S. Mashkovtseva, S. Nemrava, N.S. Perov, A.S. Semialova, I.V. Krivtsov, L.I. Isaenko, G.G. Mikhailov, R. Niewa, Ti-substituted $BaFe_{12}O_{19}$ singel crystal growth and characterization, Cryst.

Growth Des. 14 (11) (2014) 5834–5839.
[14] K.K. Mallick, P. Stepherd, R.J. Green, Magnetic properties of cobalt substituted M-type barium hexaferrite prepared by co-precipitation, JMMM 312 (2007) 418–429.
[15] M. Begard, K. Bobzin, G. Boleli, A. Hujanen, P. Lintunen, D. Lisjak, S. Gyergyek, L. Lusvarghi, M. Pasquale, K. Richardt, T. Schläfer, T. Varis, Thermal spraying of Co,Ti-substituted Ba-hexaferrite coatings for electromagnetic wave absorption applications, Surf. Coat. Technol. 203 (2009) 3312–3319.
[16] X.Z. Zhou, A.H. Morrish, Z. Yang, H.X. Zeng, Co–Sn substituted barium ferrite particles, J. Appl. Phys. 75 (1994) 5556.
[17] H.C. Frang, C.K. Ong, X.Y. Zhang, Y. Li, X.Z. Wang, Z. Yang, Low temperature characterization of nano-sized $BaFe_{12-2x}Zn_xSn_xO_{19}$ particles, JMMM 191 (1999) 277–281.
[18] G. Mendoza-Suarez, L.P. Rivas-Vazquez, J.C. Corral-Huacuz, A.F. Fuentes, J.I. Escalante-Garcıa, Magnetic properties and microstructure of BaFe11.6–2xTixMxO19 (M= Co, Zn, Sn) compounds, Phys. B Condens. Matter 339 (2003) 110–118.
[19] C.K. Ong, H.C. Fang, Z. Yang, Y. Li, Magnetic relaxation in Zn–Sn-doped barium ferrite nanoparticles for recording, JMMM 213 (2000) 413–417.
[20] H.C. Fang, Z. Yang, C.K. Ong, Y. Li, C.S. Wang, Preparation and magnetic properties of (Zn–Sn) substituted barium hexaferrite nanoparticles for magnetic recording, JMMM 187 (1998) 129–135.
[21] S. Ounnunkad, P. Winotai, Properties of Cr-substituted M-type barium ferrites prepared by nitrate–citrate gel-autocombustion process, JMMM 301 (2006) 292–300.
[22] Y. Liu, M.G.B. Drew, J. Wang, M. Zhang, Y. Liu, Preparation, characterization and magnetic properties of the doped barium hexaferrites $BaFe_{12-2x}Co_{x/2}Zn_{x/2}Sn_xO_{19}$, x=0.0–2.0, JMMM 322 (2010) 366–374.
[23] J. Slama, A. Grushkova, M. Papanova, D. Kevicka, R. Dosoudil, V. Jančárik, A. González, G. Mendoza, Magnetic properties of Me–Zr substituted Ba–hexaferrite, JMMM 272–276 (2004) 385–387.
[24] D. Mishra, S. Anand, R.K. Panda, R.P. Das, Studies on characterization, microstructures and magnetic properties of nano-size barium hexa-ferrite prepared through a hydrothermal precipitation–calcination route, Mater. Chem. Phys. 86 (2004) 132–136.
[25] Y. Liu, J. Wang, M. Hu, M. Zhang, T. Xia, Synthesis and magnetic properties of single magnetic domain hexagonal barium ferrite via sol-gel technique, Chin. J. Appl. Chem. 24 (2007) 1182–1186.
[26] D.A. Vinnik, D.A. Zherebtsov, L.S. Mashkovtseva, S. Nemrava, A.S. Semisalova, D.M. Galimov, S.A. Gudkova, I.V. Chumanov, L.I. Isaenko, R. Niewa, Growth, structural and magnetic characterization of Co- and Ni-substituted barium hexaferrite single crystals, J. Alloys Compd. 628 (2015) 480–484.
[27] D.E. Bugaris, H.-C. zurLoye, Materials Discovery by flux Crystal growth: quaternary and higher order oxides, Angew. Chem. Int. Ed. 51 (16) (2012) 3780–3811.
[28] T. Siegrist, T.A. Vanderah, Combining magnets and dielectrics: crystal chemistry in the $BaO–Fe_2O_3–TiO_2$ system, Eur. J. Inorg. Chem. 2003 (8) (2003) 1483–1501.
[29] D.A. Vinnik, D.A. Zherebtsov, L.S. Mashkovtseva, A.K. Yakushechkina, A.S. Semisalova, N.S. Perov, L.I. Isaenko, R. Niewa, Tungsten substituted $BaFe_{12}O_{19}$ single crystal growth and characterization, Mater. Chem. Phys. 29 (2015) 99–103.
[30] D.A. Vinnik, D.A. Zherebtsov, L.S. Mashkovtseva, S. Nemrava, M. Bischoff, N.S. Perov, A.S. Semisalova, I.V. Krivtsov, I.L. Isaenko, G.G. Mikhailov, R. Niewa, Growth, structural and magnetic characterization of Al-substituted barium hexaferrite single crystals, J. Alloys Compd. 615 (2014) 1043–1046.
[31] D.A. Vinnik, A. Tarasova, D.A. Zherebtsov, L.S. Mashkovtseva, S.A. Gudkova, S. Nemrava, A.K. Yakushechkina, A.S. Semisalova, L.I. Isaenko, R. Niewa, Cu-substituted barium hexaferrite crystal growth and characterization, Ceram. Intern., Submitted for publication.
[32] X. Ping, H. Xijiang, M. Wang, Synthesis and magnetic properties of $BaFe_{12}O_{19}$ hexaferrite nanoparticles by a reverse microemulsion technique, J. Phys. Chem. C 111 (2007) 5866–5870.
[33] Y. Naito, K. Suetake, Application of ferrite to electromagnetic wave absorber and its characteristics, IEEE Trans. Microware Theor. Tech. MTT 19 (1971) 65–72.
[34] K. Ishino, Y. Narumiya, Am. Ceram. Soc. Bull. 66 (1987) 1469–1474.
[35] J.Y. Shin, J.H. Oh, The microwave absorbing phenomena of ferrite microwave absorbers, IEEE Trans. Magn. 29 (1993) 3437–3439.
[36] X. Tang, Y. Yang, K. Hu, Structure and electromagnetic behavior of $BaFe_{12-2x}(Ni_{0.8}Ti_{x0.7})_xO_{19}$ in the 2–12 GHz frequency range, J. Alloys Compd. 477 (2009) 488–492.
[37] R. Tholkappiyan, K. Vishista, Synthesis and characterization of barium zinc ferrite nanoparticles: working electrode for dye sensitized solar cell applications, Third Fourth Gener. Sol. Cells 106 (2014) 118–128.
[38] A. Ghasemi, A. Hossienpour, A. Morisako, X. Liu, A. Ashrafizadeh, Investigation of the microwave absorptive behavior of doped barium ferrites, Mater. Des. 29 (1) (2008) 112–117.
[39] Y. Liu, M.G.B. Drew, Y. Liu, J. Wang, M. Zhang, Preparation, characterization and magnetic properties of the doped barium hexaferrites $BaFe_{12-2x}Co_{x/2}Zn_{x/2}Sn_xO19$, x=0.0–2.0, JMMM 322 (7) (2010) 814–818.
[40] F. Wei, M. Lu, Z. Yang, The temperature dependence of magnetic properties of Zn–Ti substituted Ba-ferrite particles for magnetic recording, JMMM 191 (1–2) (1999) 249–253.
[41] A. Gonzalez-Angeles, G. Mendoza-Suarez, A. Gruskova, M. Papanova, J. Slama, Magnetic studies of Zn–Ti-substituted barium hexaferrites prepared by mechanical milling, Mater. Lett. 59 (1) (2005) 26–31.
[42] D.A. Vinnik, D.A. Zherebtsov, L.S. Mashkovtseva, Growing doped barium ferrite single crystals using the flux method, Dokl. Phys. Chem. 449 (2013) 39–40.
[43] D.A. Vinnik, O.S. Kolodkina, D.A. Zherebtsov, V.V. Dyachuk, Growing the $PbTiO_3$ from solution, Bull. S. Ural. State Univ. Metall. Ser. 19 (2012) 19–21.
[44] D.A. Vinnik, L.S. Mashkovtseva, D.A. Zherebtsov, V.V. Dyachuk, G.G. Mikhailov, Growing of barium ferrite crystals from a solution, Bull. S. Ural. State Univ. Metall. Ser. 36 (253) (2011) 41–44.
[45] A.M. Balbashov, S.K. Egorov, Apparatus for growth of single crystals of oxide compounds by floating zone melting with radiation heating, J. Cryst. Growth 52 (1981) 498–504.
[46] W.D. Townes, J.H. Fang, A.J. Perrotta, The crystal structure and refinement of ferromagnetic barium ferrite, $BaFe_{12}O_{19}$, Z. Krist. 125 (1967) 437–449.
[47] R.D. Shannon, Revised effective ionic radii and systematic studies of interatomic distances in halides and chalcogenides, Acta Crystallogr. A32 (1976) 751–767.
[48] F.-Z. Mou, J.-G. Guan, Z.-G. Sun, X.-A. Fan, G.-X. Tong, In situ generated dense shell-engaged Ostwald ripening: a facile controlled-preparation for $BaFe_{12}O_{19}$ hierarchical hollow fiber arrays, J. Solid State Chem. 183 (2010) 736–743.
[49] V. Pillai, P. Kumar, M.S. Multani1, D.O. Shah, Structure and magnetic properties of nanoparticles of barium ferrite synthesized using microemulsion processing, Coll. Surf. A 80 (1993) 69–71.
[50] K. Watanabe, Growth of minute barium ferrite single crystals from a Na_2O-B_2O_3 flux system, J. Cryst. Growth 169 (1996) 509–518.
[51] P. Wartewig, M.K. Krause, P. Esquinazi, S. Roslor, R. Sonntag, J. Magn. Magn. Mater 192 (1999) 83.
[52] Z. Yang, C.S. Wang, X.H. Li, H.X. Zeng, (Zn, Ni, Ti) substituted barium ferrite particles with improved temperature coefficient of coercivity, Mater. Sci. Eng. B90 (2002) 142–145.
[53] L. Shlyk, S. Strobel, E. Rose, R. Niewa, $BaZnRu_5O_{11}$: novel compound with frustrated magnetic lattice based on distorted kagome networks, Solid State Sci. 14 (2012) 281–286.
[54] L. Shlyk, S. Strobel, Th Schleid, R. Niewa, Ruthenate-ferrites $AMRu_5O_{11}$ (A = Sr, BaM = Ni, Zn): distortion of kagome nets via metal–metal bonding, Z. Krist. 227 (2012) 545–551.